Electronically Supplementary Information (ESI)

Advanced Sodium Storage Property in Exfoliated MoO_3 Anode: The Stability and Performance Improvement by *in-situ* Impedance Mapping

Amlan Roy[#], Prasit Kumar Dutta[#] and Sagar Mitra*

Electrochemical Energy Laboratory, Department of Energy Science and Engineering,

Indian Institute of Technology, Bombay, Powai, Mumbai 400076, India

AUTHOR INFORMATION

Corresponding Author: sagar.mitra@iitb.ac.in

Tel: +91-222576-7849

1. Introduction

In the main draft, we have attached the main highlights of the whole project. Whereas in the supporting information, we have attached the experimental supports.

2. Choosing Color Combination

In this work, a simple RGB color combination has been used to distinguish three materials: blue for B-MoO_3, red for E-MoO_3 and green for rE-MoO_3.

3. Preparation of B-MoO_3, E-MoO_3 and rE-MoO_3 Composite

3.1. Synthesis of GO and r-GO

Graphene oxide (GO) was synthesized by using modified Hammers method.[1] Briefly, the mixture of graphite flakes (1g) and $NaNO_3$(1g) was added to 50mL concentrated H_2SO_4 (in 500 ml beaker at 0-5 ℃) and stirred for 30min. to produced graphite intercalated compound (GIC). Then 6 gm of solid $KMnO_4$ was slowly added to the GIC reaction mixture and gently stirred for 1hr. to allow the oxidation process. The mixture was then diluted with 250 ml of water. After 30 min, 15 ml of 30% of H_2O_2 was drop-wisely added until the gas evolution was ceased. The residue of exfoliated graphite oxide was thoroughly washed with DI water and 10% dilute HCl. After that, the precipitate was collected and dried in vacuum oven at 50℃. Thermal reduction process was followed to reduce the graphene oxide paper. In a typical process, 0.15 gm of GO paper was heated in a tubular furnace at 850 ℃ for 30 min (heating rate 7 ℃ min^{-1}) under an inert atmosphere to prepare rGO.

3.2. Synthesis of α-MoO_3

α-MoO_3 nano-belts (B-MoO_3) were synthesized by hydrothermal method.[2] In this procedure,8.2 millimoles of sodium molybdate dihydrate (Na_2MoO_4,$2H_2O$) was dissolved in 30 ml DI water and stirred for 30 min. In acidification technique, 5 ml of perchloric acid (5 M) was added gradually to the solution under constant stirring. After 45 min., a white color turbid solution was observed and it was transferred to Teflon-lined stainless-steel autoclave and kept

for 24 hr at 180 ℃. Then the product was washed several times with the copious amount of water/ethanol mixture solution, the white color precipitate was dried in hot air oven (60 ℃ for 12 hr). To improve the crystallinity, the dried sample was heated up to 500 ℃ in inert Argon atmosphere.

3.3. Exfoliation of α-MoO_3

As prepared α-MoO_3 (1gm ml^{-1}) was added to 2.0 mL of Benzene and was continuously stirred for 1hr. Aging step was done by keeping the solution 2hr without any disturbance. After that, the thick solution was ground using a mortar and pestle for 120 min. While grinding, an extra 1.0 mL of solvent was also added in 2.0 mL of solution to maintain the viscosity. The powder was then kept for drying in a vacuum oven (~500 mm Hg) at 80 °C for overnight. The dried sample was dispersed in isopropyl alcohol and water mixture (1:1 v/v) at a concentration of 2 mg ml^{-1} by ultrasonication for 5hr. The dispersion was cooled by ice water during sonication. In sonication process, α-MoO_3 gradually exfoliated into sheets (E-MoO_3) via intercalation of IPA/water molecules. Afterward, the solution was centrifuged for 30 min at 2000 rpm (Eppendorf centrifuge-5804) to remove the aggregates. and the supernatant was collected. To make a α-MoO_3 electrode, the supernatant was centrifuged at 8000 rpm for 10 min. to collect exfoliated α-MoO_3 and dried overnight for 12hr in a vacuum oven at 100 °C.

3.4. Preparation of rE-MoO_3

Two solutions: (i) E-MoO_3 in N-methyl pyrolidine (2 mg ml^{-1}) and (ii) as-prepared rGO in N-methyl pyrolidine (0.25 mg ml^{-1}) were mixed in a beaker. Nearly 70 ml mixture (50 ml of solution i and 20 ml of solution ii) was prepared in one batch which was further bath sonicated for 30 min and centrifuged for 10 min. In the next step, the precipitate was collected in a petri dish which was subjected to air dry in hot air oven, kept overnight at 60 °C.

While making the electrode, 60% of rE-MoO_3 was used as active material. In 60%, used rGO percentage was 5%. Hence, 3 weight percent of rGO (compared with overall electrode mass) was used to evaluate the study.

4. Proof of Morphology Change after Cycling by *ex-situ* SEM

The morphology (Figure S1a) of the material has found (*ex-situ* SEM) altered after 5 successive potentiostatic cycles cycled at a sweep rate of 50 μv s^{-1}. However, this change was only observed on the front surface, not on the current collector side (Figure S1d). The overall process of *ex-situ* SEM characterization has been shown in Figure S1c. Hence, we have assessed that the capacity can be improved, if we can synthesis the similar morphology (comparison of Figure S1a and S1b). In the process of agitation, after 2 hours, similar kind of flat morphology has been observed. In the next step, a chemical path has been followed to exfoliate the material contouring a reduced size.

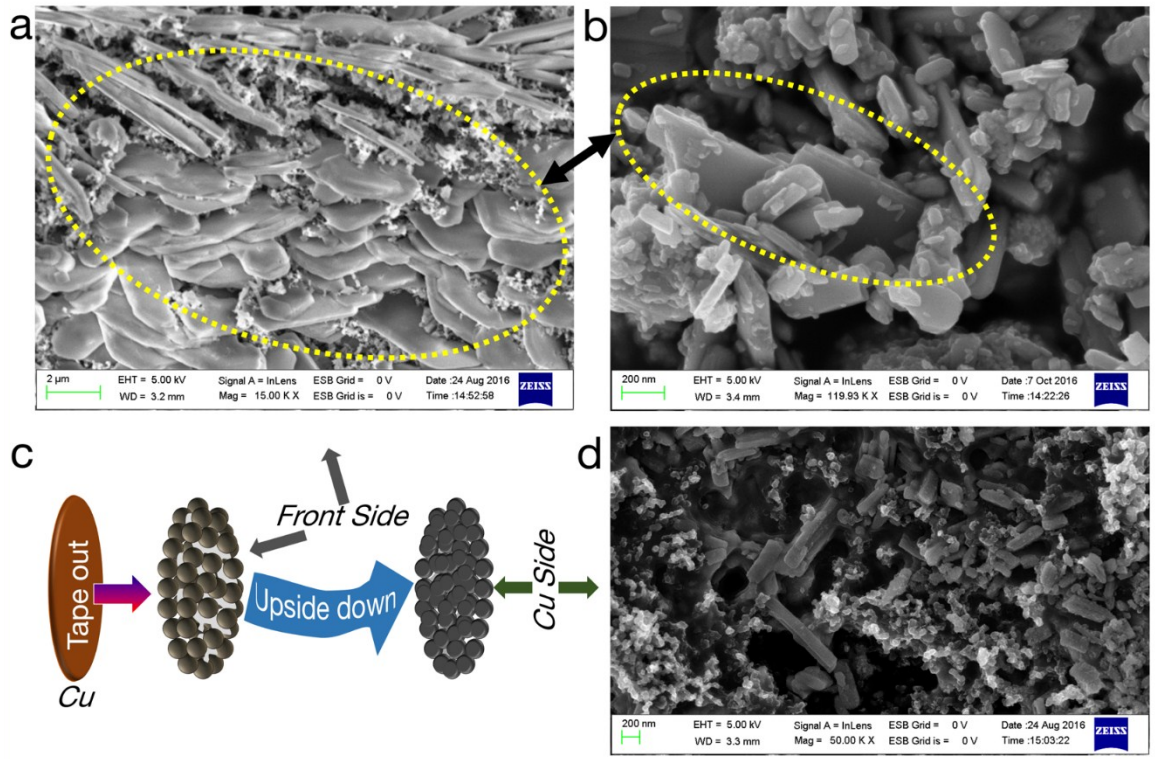

Figure S1: (a, d) *Ex-situ* images of cycled electrode, (b) SEM image of agitated B-MoO_3 with (c) the process of tape out.

5. Support for the Mechanism of Exfoliation

Here, we have mapped the mechanism of exfoliation via two pathways: agitation assisted chemical exfoliation and direct exfoliation of the material (Figure S2). It has been found that the agitation assisted path is quite rapid to get an exfoliated few-layered material whereas, the direct chemical path is quite slow in compare to the previous one. Also, the information of mechanism has been explicitly understood from the SEM images taken at the different time of the experiment. The agitation assisted path helps to make crack onto the as-prepared nanobelts whereas the direct path only controls the exfoliation from the edge.

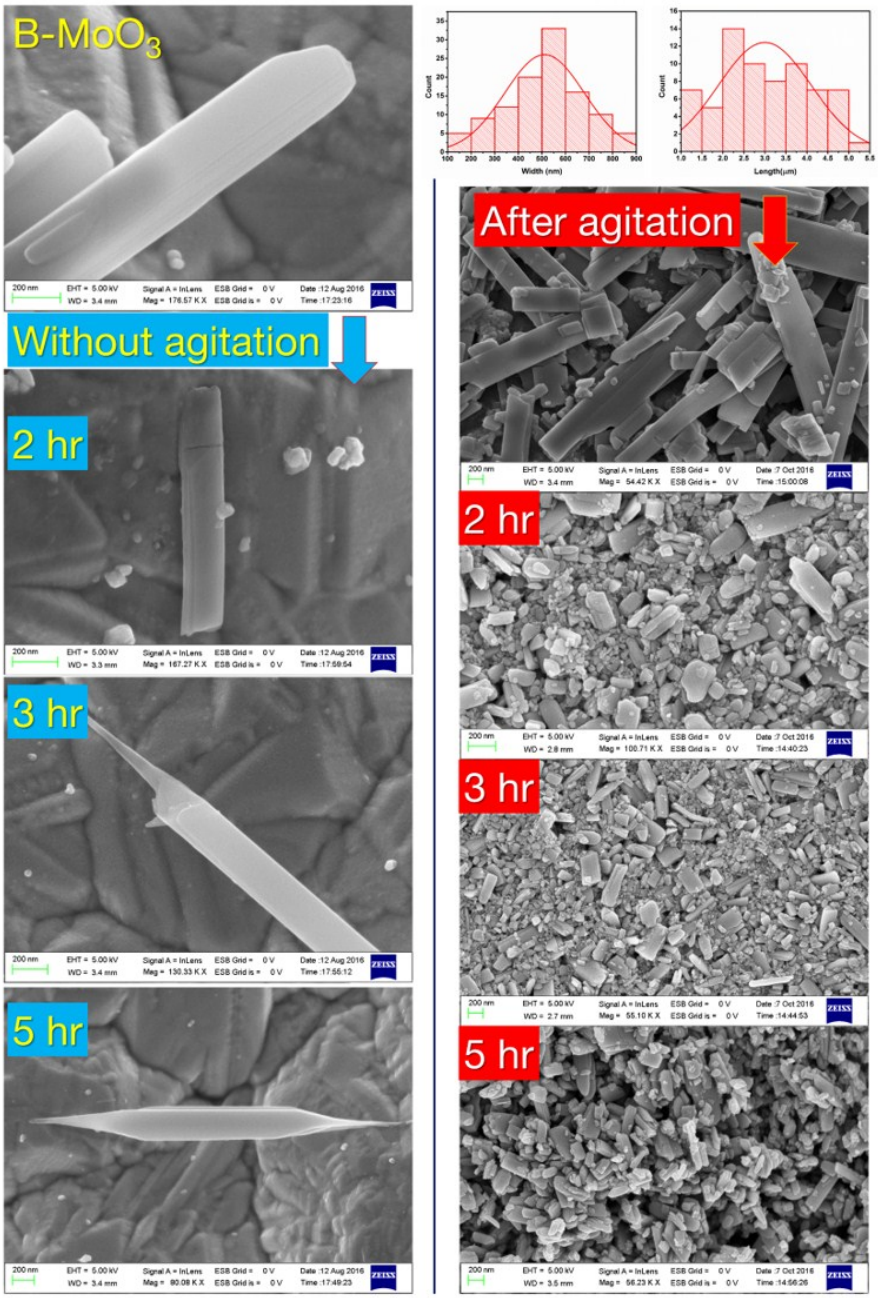

Figure S2: Exfoliation process with and without agitation, with width and length measurements for B-MoO_3.

6. X-ray Diffraction Study

The distinguishable X-ray diffraction pattern of B-MoO3 from JCPDS data reflects that the peak intensities are quite high for (0 k 0) directions (Figure S3a). This proofs for the crystal growth occurred perpendicular to (0 k 0) direction. After exfoliation, the peak intensities along (0 k 0) direction reduces significantly. A peak broadening has been observed explicitly form

the XRD pattern (Figure 3b). In a nutshell, the reduction of peak intensities depicts the exfoliation of the nanobelts (along *b*-direction) whereas broadening reflects the breakage (perpendicular to *b*-direction).

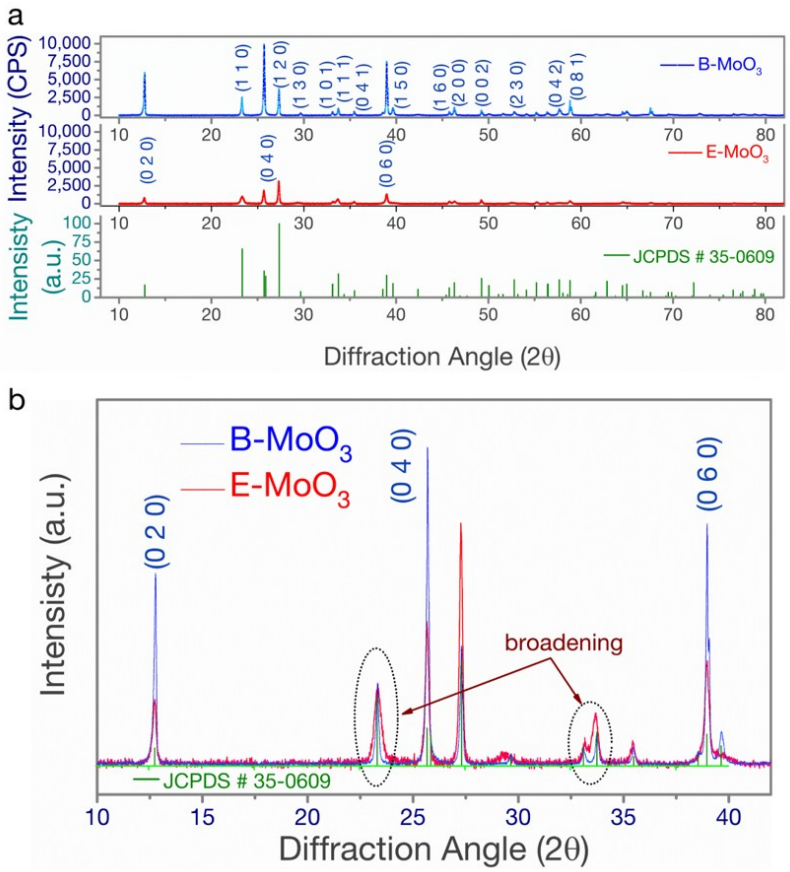

Figure S3: X-ray diffraction pattern showing (a) marked crystal planes for α-MoO_3 (b) peak broadening in XRD pattern.

7. Discussion on AFM

Here, we are providing the optical image observed through AFM. Here, the double layer thickness is ~1.4 nm. Two particles were matched to interpret the thickness of the particles.

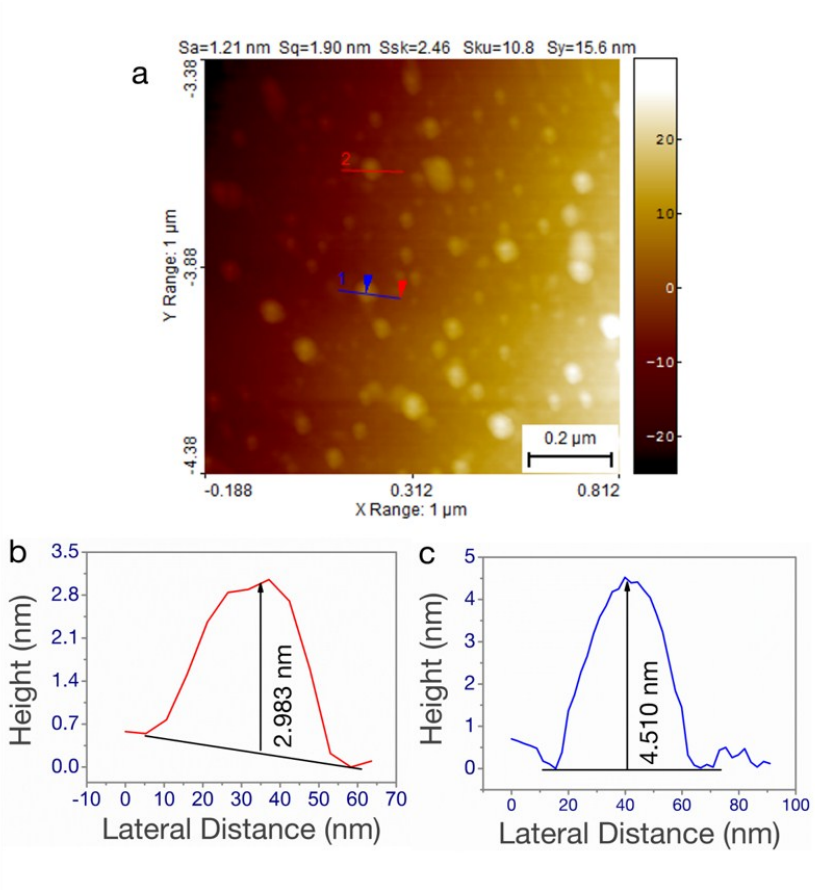

Figure S4: (a) AFM images at (b, c) two different location.

8. Confocal Raman Spectra

The used instrument is having a resolution of 0.5 cm^{-1}. Here, the overall spectra have been shown. The highest intensity peaks were plotted separately to understand the effect of morphology. The average Gaussian nature of the peaks shifts slightly on the lower wavenumber direction for B-MoO_3 conveying a change in morphology to E-MoO_3. It reflects that the B-MoO_3 is in a shape of rod-like whereas the E-MoO_3 shapes less towards that morphology. However, we expected more shift from Raman.

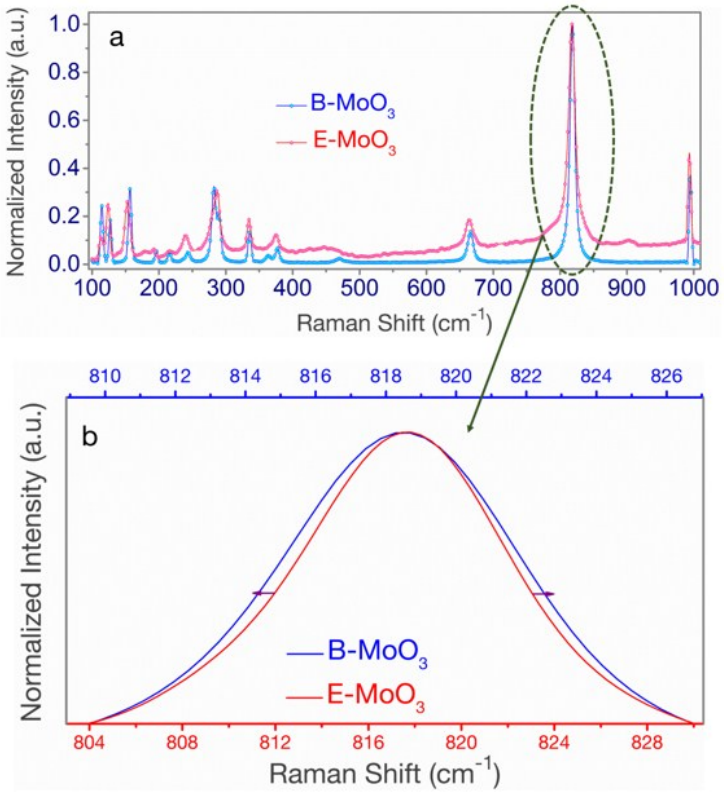

Figure S5: (a) Broad laser Raman confocal spectra and (b) effect of morphology for B-MoO_3 and E-MoO_3.

Along with, few more peaks shifts are incorporated below which are not incorporated in the main draft.

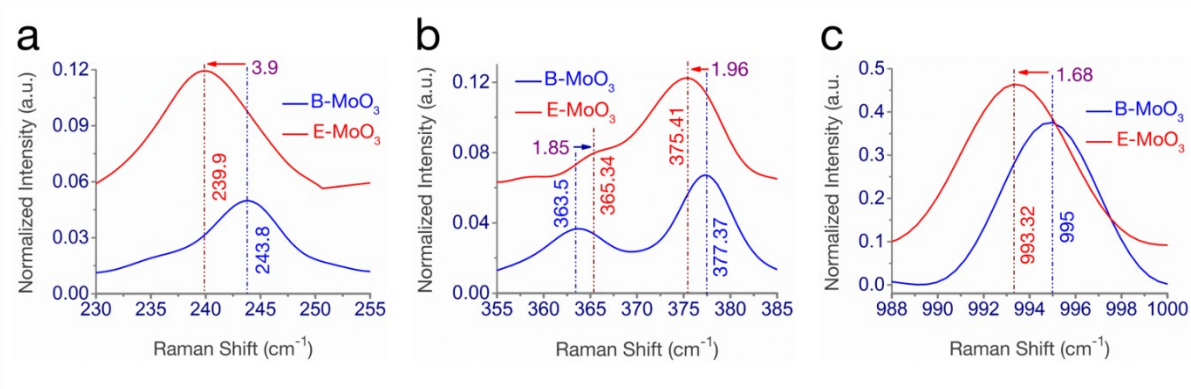

Figure S6: (a-c) Peak shifts for B-MoO_3 and E-MoO_3.

9. Detailed Discussion on *in-situ* Impedance Mapping

In the main draft, we have claimed that a new experiment on impedance has been performed which helps us to scavenge the interfacial stability of the systems. Here we have plotted three different impedance curves. The first two (Figure S7, a-b) correspond to the Bode plots and the Figure S7 c corresponds to Black impedance for B-MoO_3 mapping. Form Black impedance, we have precisely taken the points where the big semi-circles end. The points lie near phase angle of 20 degrees in the particular graph (Figure S7 c). An initial voltage stability for E-MoO_3 and rE-MoO_3 were observed (main draft, Figure 4 c, inset) which may depict wetting of electrolyte for used electrodes. However, these electrodes wet very faster in comparison to B-MoO_3. Hence, the OCV gets stabilized much faster than B-MoO_3. For preparing Figure 4f, the points were taken using Black impedance spectra and fitted via Pearson VII technique using Origin software.

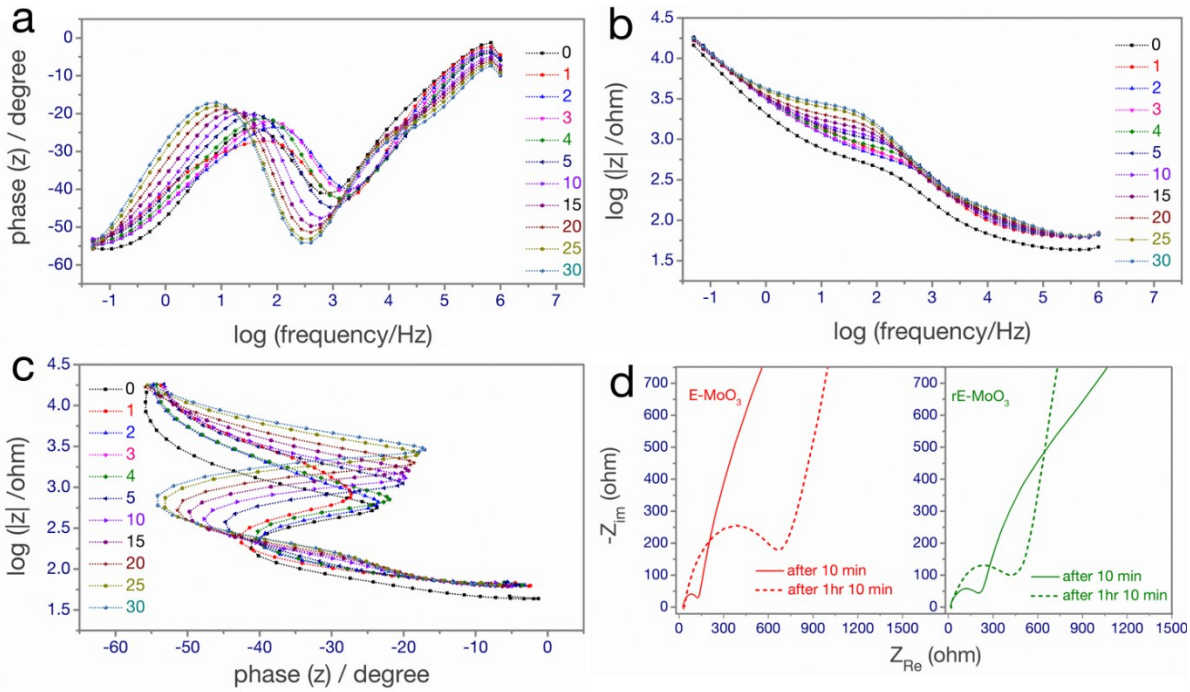

Figure S7: (a, b) Bode plots, (c) Black impedance for B-MoO_3, (d) and change in PEIS after 1 hr for E-MoO_3 and rE-MoO_3.

We feel that the wetting of B-MoO_3 takes more time than the other two electrodes resulting a prominent hump in the Hz-time plot (main draft, Figure 4 d). To endorse the intuition of wetting

of electrode we have compared digital images (captured using iPhone 5s, 8-megapixel iSight camera) of B-MoO_3 electrodes, before and after the wetting experiment. As prepared B-MoO_3 is off-white in color. Hence, the electrode looks like gray in color. Whereas the electrode looks darker after the mapping experiment. However, it is difficult to compare the same images for E-MoO_3 and rE-MoO_3 as those electrodes are very dark in color.

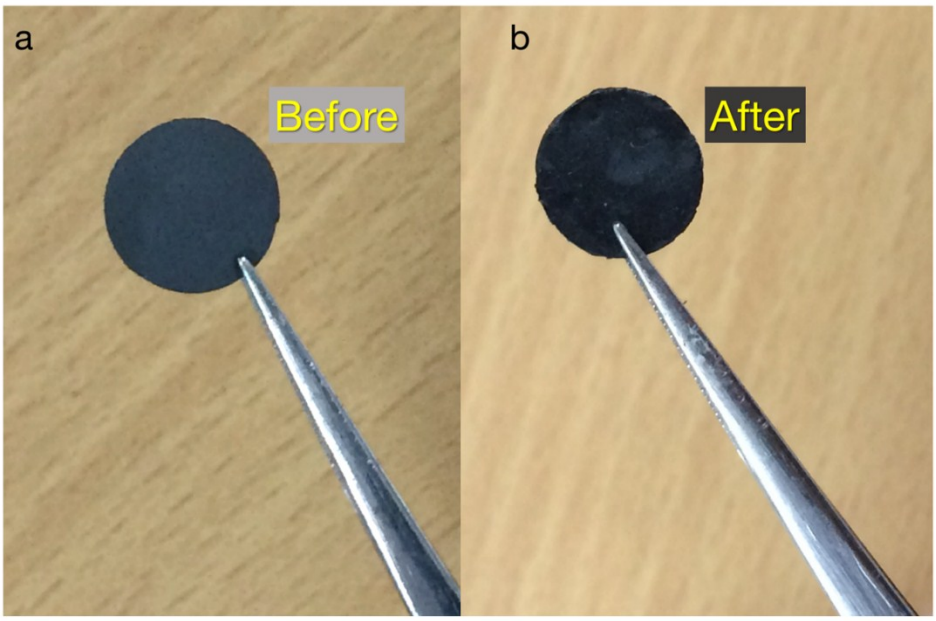

Figure S8: B-MoO_3 electrode (a) before and (b) after the mapping experiment.

To support the lowering of OCV a similar PEIS-mapping test were performed with the prepared rGO sample. For this experiment, an electrode was composed with rGO, Super C-65 and cmc taking them at a weight ratio of 8:20:20. It has been found that the OCV was stabilized near 2.2 V.

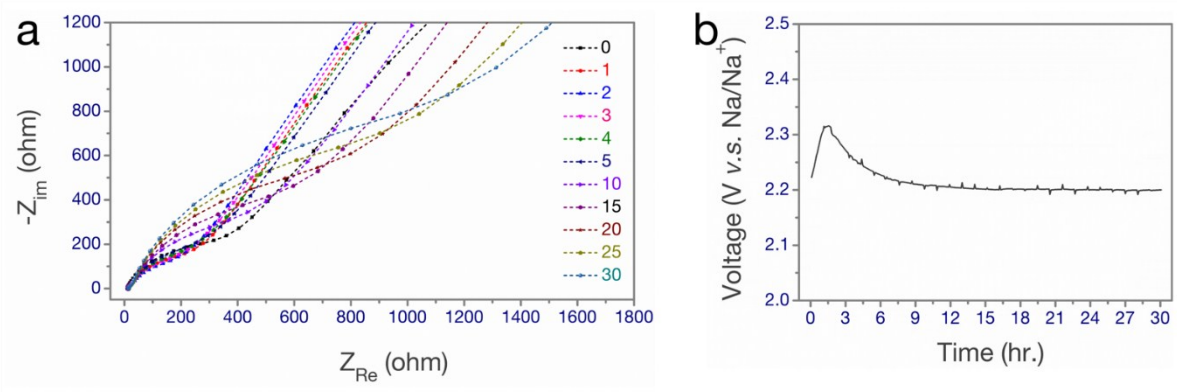

Figure S9: (a) PEIS-mapping and (b) OCV stability curve for rGO-Super C electrode.

10. Effect of Relaxation

Two cells were compared for this study. One of the freshly prepared cells were subjected to discharge-recharge; in contrast, the other one was relaxed for ~30 hours. Both cells were cycled at a fixed current rate of 50 mA g^{-1}. The initial discharge was same for both of the cells whereas a distinguishable capacity improvement was achieved after giving relaxation. A 100 cycle performance has been compared below.

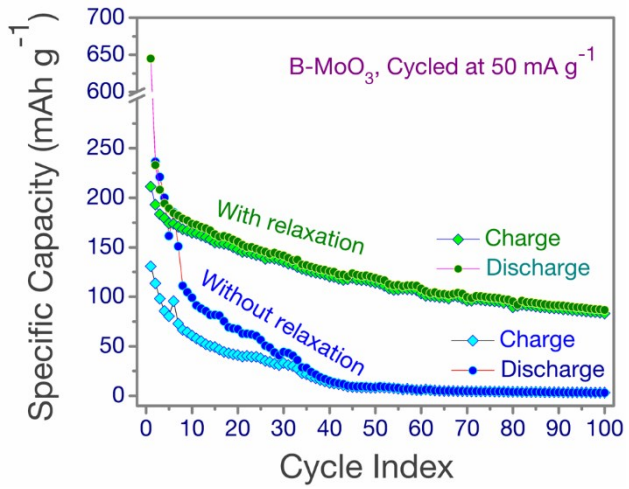

Figure S10: Effect of relaxation after cell fabrication for B-MoO_3.

11. rGO-MoO_3 Composite

Figure S11a shows the 2D rGO sheets observed through SEM. From X-Ray diffraction patterns (Figure 11b), it is quite distinguishable that GO got reduced sufficiently into rGO sheets. Onto this 2D rGO sheets, E-MoO_3 was anchored to prepare the rE-MoO_3. Figure S11c reflects a well-defined anchoring of exfoliated MoO_3 onto rGO sheets. Figure S11d decribes the TGA data for E-MoO3 and rE-MoO3 composite, performed at a heating rate of 10 °C min^{-1}.

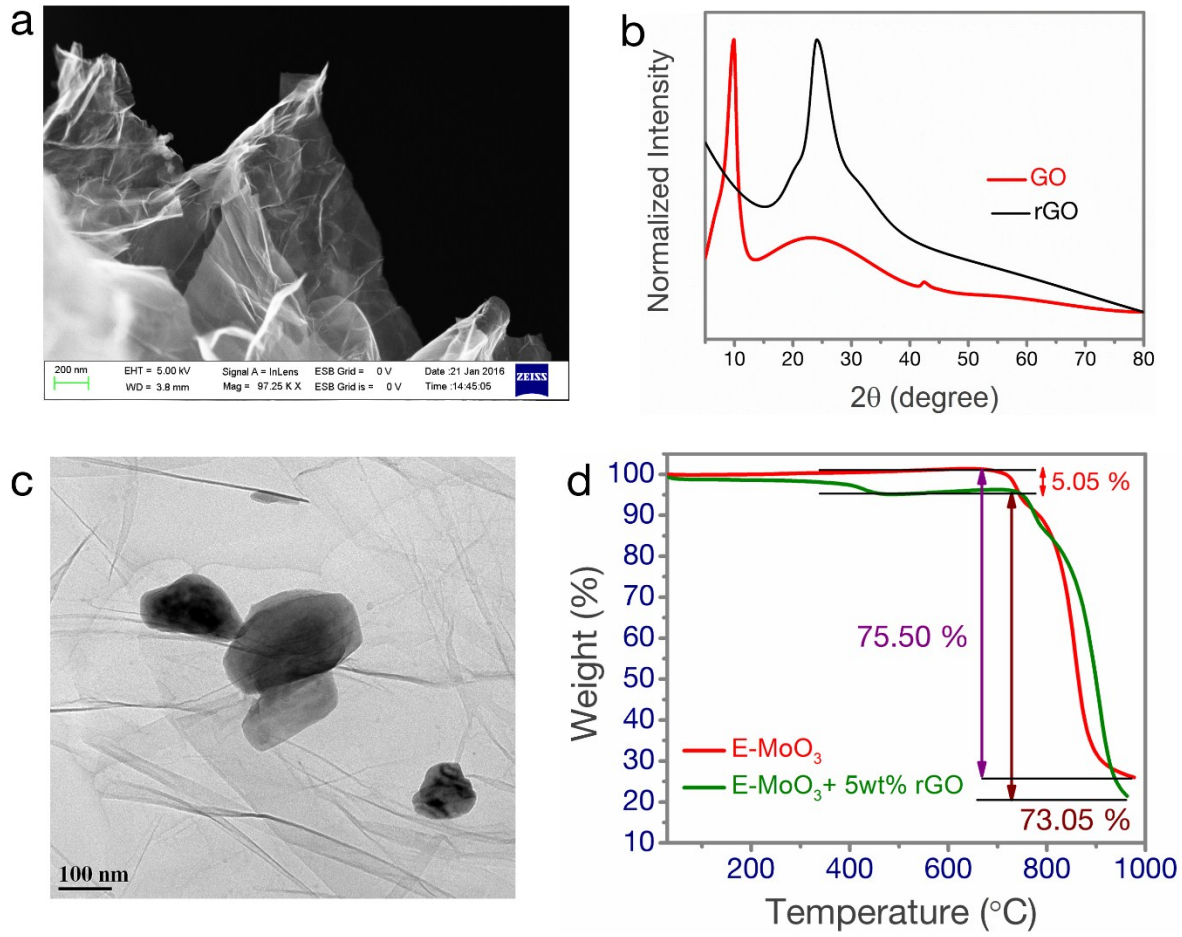

Figure S11: (a) SEM image of rGO, (b) XRD of GO, rGO (c) TEM image of rE-MoO_3 and (d) TGA of the composite.

12. Cycling Performances

For assessing the reaction positions, a slow scan cyclic voltammetry was performed at a fixed sweep rate of 50 μv s^{-1}. The area under the curve was increased from B-MoO_3 (Figure S12a) to E-MoO_3 (Figure S12b). This signifies an improvement in power density. This similar improvement found further in case of rE-MoO_3 (Figure S12c). Discharge-recharge profile for rE-MoO_3 has been plotted (Figure S12d) which shows a decent continuation of reaction paths till 100 cycles. The dQ|dV curve (Figure S12 d, inset) shows the reversibility due to conversion reaction still present till 100 cycles which is an excellent behavior for the rGO-MoO_3 composite. The peak ~0.3 V depicts the Na_2O formation and the broad peak 0.3-0.9 reflects the

reverse reaction. The areal density of the rE-MoO_3 electrode (used in the report) was 1.65 mg cm^{-2}. The thickness of the electrode was 20 µm (used Cu foil was 14 µm and the overall thickness of electrode with Cu foil was 34 µm). Hence, overall loading was 825 mg cm^{-3}.

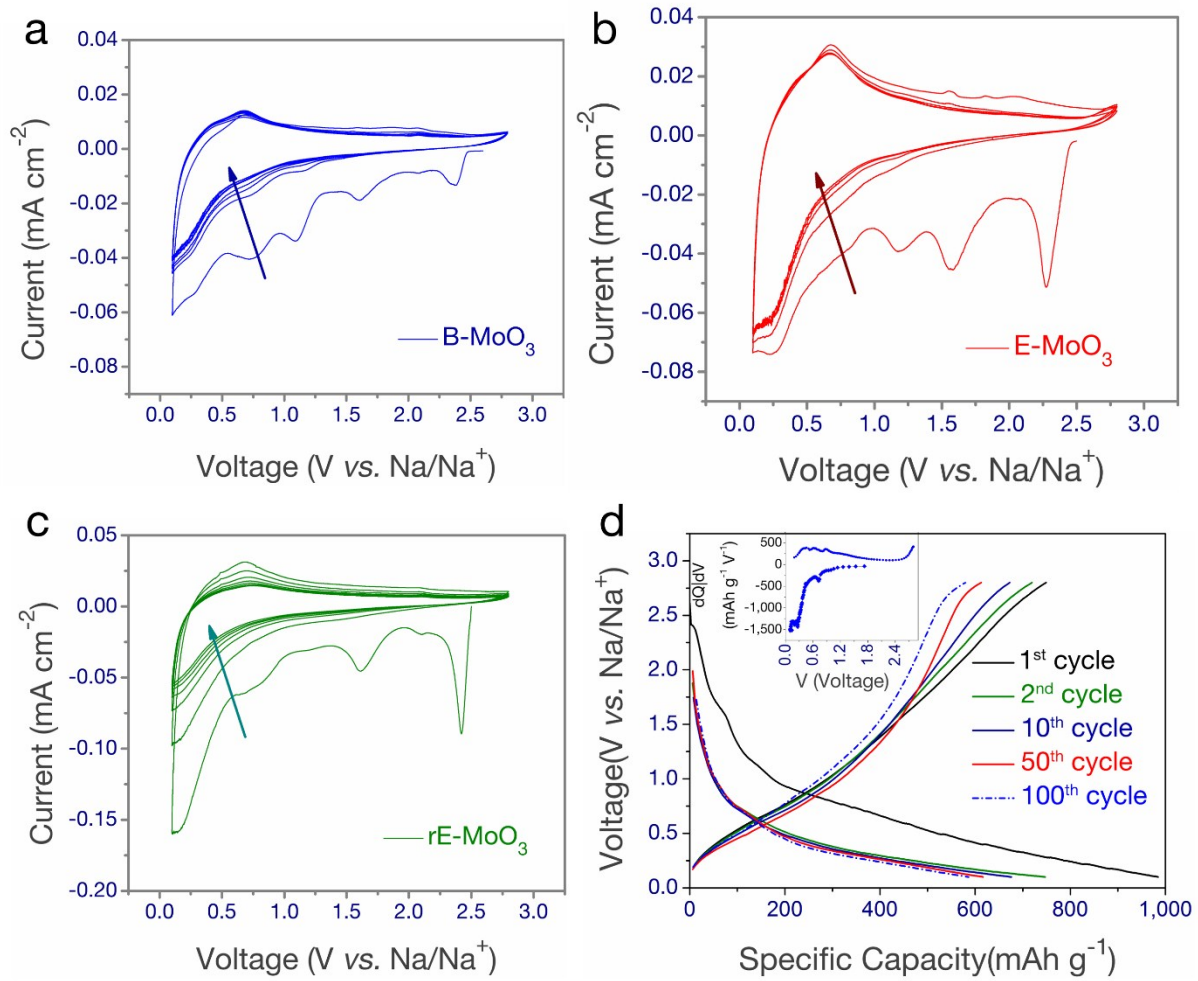

Figure S12: (a-c) Cyclic voltammograms of B-MoO_3, E-MoO_3 and rE-MoO_3. (d) Discharge-recharge profiles for rE-MoO_3. Inset: dQ|dV curve.

Only, the prepared rGO was cycled to demonstrate the capacity contribution from the material. Here, 80% of rGO was used with 20% cmc to prepare the electrode. A stable capacity contribution ~140 mAh g^{-1} has been observed (Figure S13a) from the electrode while cycled at 50 mA g^{-1} current rate. Also, a comparison of different rGO composites has been compared in figure S13b.

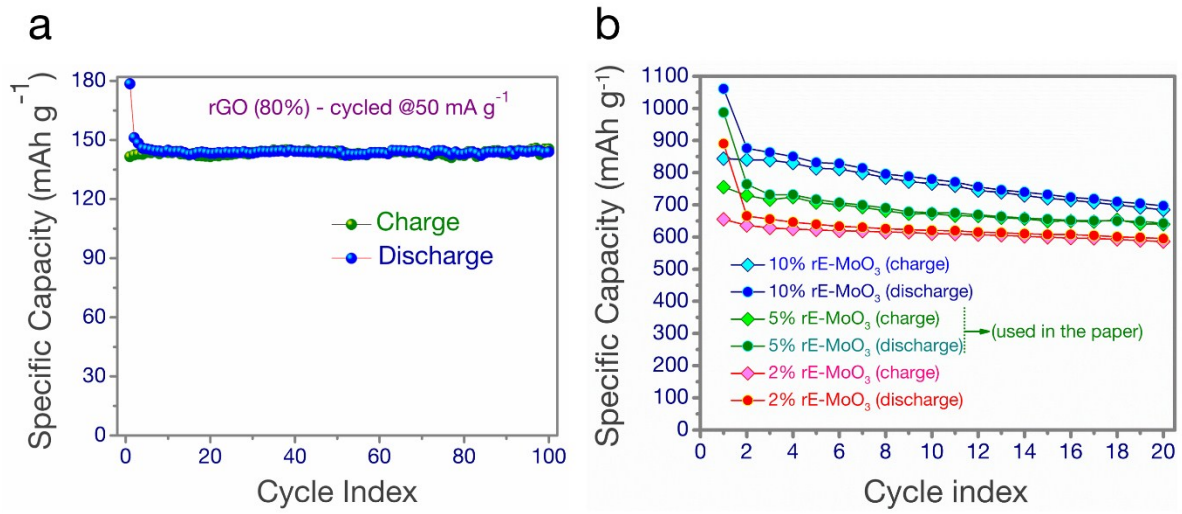

Figure S13: (a)Durability of rGO over 100 cycles and (b) comparison of different rGO-MoO_3 compsite, cycled at 50 mA g^{-1} current rate.

13. Cycling Performance

Here, we have compared our current study with the existing literature. Figure S14 shows the comparison curve at different C-rates. Ref in the curve correspond to the used references in the main paper.

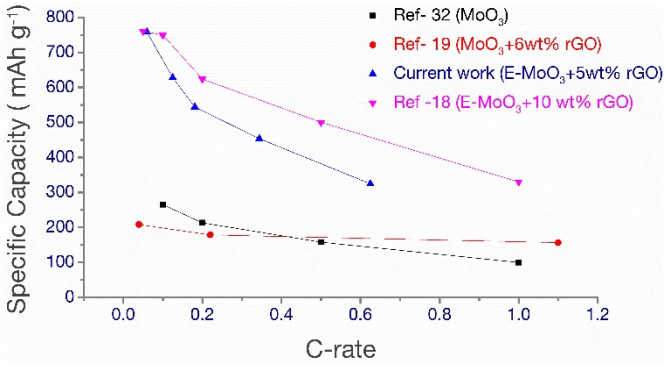

Figure S14: Comparison curve for different reports on MoO_3 anodes for sodium-ion batteries.

References

[1] W. S. Hummers, R. E. Offeman, *J. Amer. Chem. Soc.* **1958**, *80*, 1339.

[2] U. K. Sen, S. Mitra, *RSC Adv.* **2012**, *2*, 11123.